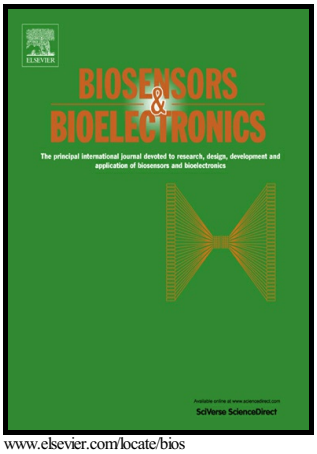

www.elsevier.com/locate/bios

Unlocked Nucleic Acids for miRNA Detection Using Two Dimensional Nano-Graphene Oxide

Neil M. Robertson, Amy E. Toscano, Vincent E. LaMantia, Mustafa Salih Hizir, Muhit Rana, Mustafa Balcioglu, Jia Sheng, Mehmet V. Yigit

PII: S0956-5663(16)30164-6
DOI: http://dx.doi.org/10.1016/j.bios.2016.02.058
Reference: BIOS8494

To appear in: *Biosensors and Bioelectronic*

Received date: 11 November 2015
Revised date: 22 February 2016
Accepted date: 23 February 2016

Cite this article as: Neil M. Robertson, Amy E. Toscano, Vincent E. LaMantia, Mustafa Salih Hizir, Muhit Rana, Mustafa Balcioglu, Jia Sheng and Mehmet V Yigit, Unlocked Nucleic Acids for miRNA Detection Using Two Dimensional Nano-Graphene Oxide, *Biosensors and Bioelectronic* http://dx.doi.org/10.1016/j.bios.2016.02.058

Unlocked Nucleic Acids for miRNA Detection Using Two Dimensional Nano-Graphene Oxide

Neil M. Robertson[†], Amy E. Toscano[†], Vincent E. LaMantia[†], Mustafa Salih Hizir[†], Muhit Rana[†], Mustafa Balcioglu[†], Jia Sheng[†] and Mehmet V. Yigit[†, ‡, *]

†Department of Chemistry,

University at Albany, State University of New York,

1400 Washington Avenue, Albany, New York 12222, United States

‡The RNA Institute,

University at Albany, State University of New York,

1400 Washington Avenue, Albany, New York 12222, United States

*Correspondence:

Tel: (1) 518-442-3002

myigit@albany.edu

Abstract

In this study we have used unlocked nucleic acids (UNAs) to discriminate a breast cancer oncomiR from two other miRNAs in the same RNA family using two-dimensional graphene oxide nanoassemblies. Fluorescently labeled single stranded probe strands and graphene oxide nanoassemblies have been used to detect miR-10b and discriminate it from miR-10a, which differs by only a single nucleotide (12^{th} base from the 5' end), and miR-10c, which differs by only two nucleotides (12^{th} and 16^{th} bases from the 5' end). We have determined the discrimination efficacy and detection capacity of a DNA probe with two inserted UNA monomers (UNA_2), and compared it to the DNA probe with two purposefully inserted mutations (DNA_{M2}) and full complementary sequence (DNA_{full}). We have observed that UNA_2 is 50 times more powerful than DNA_{full} in discriminating miR-10b from miR-10c while generating an equally high fluorescence signal. This fluorescence signal was then further enhanced with the use of the highly specific endonuclease *dsDNase* for an enzymatic amplification step. The results demonstrate that the underutilized UNAs have enormous potential for miRNA detection and offer remarkable discrimination efficacy over single and double mismatches.

Keywords: Unlocked nucleic acid, graphene, microRNA (miRNA), nanoparticle, DNA, biosensor

Highlights:

- Incorporation of the Unlocked Nucleic Acids (UNAs) leads to an increase in discrimination efficacy without sacrificing signal generation.
- Over a 70 fold increase in specificity was observed when discriminating miR-10b from miR-10c, which differs by only two nucleotides.
- Incorporation of the *dsDNase* enzyme into the graphene oxide-based detection mechanism amplifies the signal with target miRNA without influencing the background signal.

1. Introduction

Unlocked Nucleic Acids (UNAs) are acyclic analogues of DNA and RNA molecules in which the bond between the C2' and C3' atoms of the ribose ring has been cleaved (Langkjaer et al. 2009). The UNA is in direct contrast to the Locked Nucleic Acid (LNA), which has gained significant attention recently due to its ability to improve the hybridization efficacy of oligonucleotides and stability of the duplexes (Rana et al. 2014a; Rana et al. 2014b; Yigit et al. 2013). The incorporation of LNA modifications into DNA or RNA strands increases the melting temperature about 3 °C per LNA monomer and offers better resistance against nuclease degradation (Vester and Wengel 2004; You et al. 2006). For this reason LNA technology has been extensively used for *in vivo* miRNA research (Elmen et al. 2008). The key of the LNA activity is the presence of the methylene bridge between the 2'-Oxygen and 4'-Carbon of the ribose sugar, which locks the ring into the specific C3'-*endo* configuration (Campbell and Wengel 2011), **Scheme 1a**. Opposite this, the key of the UNA is the loss of the bond between the C2' and C3' atoms, which adds enhanced flexibility relative to a native oligonucleotide (Pasternak and Wengel 2011). Incorporation of the UNA monomers has the reverse effect on duplex stability. Insertion of a single UNA base in a DNA:DNA, RNA:RNA or DNA:RNA duplex can decrease the melting temperature up to 10 °C (Jensen et al. 2008; Nielsen et al. 1995; Pasternak and Wengel 2010). This decrease in the melting temperature and destabilization of the duplex have been long overlooked since general interest has been on improving the duplex stability rather than worsening it (Campbell and Wengel 2011). However the underutilized features of UNAs could be very useful for addressing particular biomedical challenges. Here we have used the aforementioned properties of UNAs for detecting a specific miRNA, over-expressed in metastatic breast cancer, and discriminated it from two miRNAs with single and double nucleotide differences. In order to do that, two-dimensional nano-graphene oxide (nGO) has been used as the biosensing platform due to its fascinating properties at the bio-nano interface.

Two-dimensional materials have attracted remarkable attention recently due their potential use in device engineering or biosensor development (Butun et al. 2015; Mai et al. 2014; Ocsoy et al. 2013; Ozturk et al. 2015; Parlak et al. 2014; Parlak et al. 2015; Zhu et al. 2014). nGO is a one-atom-thick two-dimensional carbon material with a honeycomb structure (Allen et al. 2010; Dreyer et al. 2010; Geim 2009). Physical and electronic properties of nGO have been studied

extensively for its potential applications in a wide range of fields (Balci et al. 2015; Guo et al. 2014; Parlak et al. 2013). A number of its applications in environmental, biological and biomedical studies have been demonstrated (Chung et al. 2013). We and others have used it for the detection of cellular and circulating miRNAs to address several biomedical challenges (Balcioglu et al. 2013; Hizir et al. 2014; Robertson et al. 2015a; Robertson et al. 2015b). To accomplish miRNA detection using nGO, two core properties of graphene have been used, **Scheme 1b**. First, graphene oxide can adsorb short single stranded (ss) oligonucleotides (probes) due to aromatic stacking, hydrogen bonding, hydrophobic interactions, and van der Waals forces between the graphene surface and the nucleobases, however double stranded oligonucleotides do not bind to the graphene surface (Rana et al. 2014a).

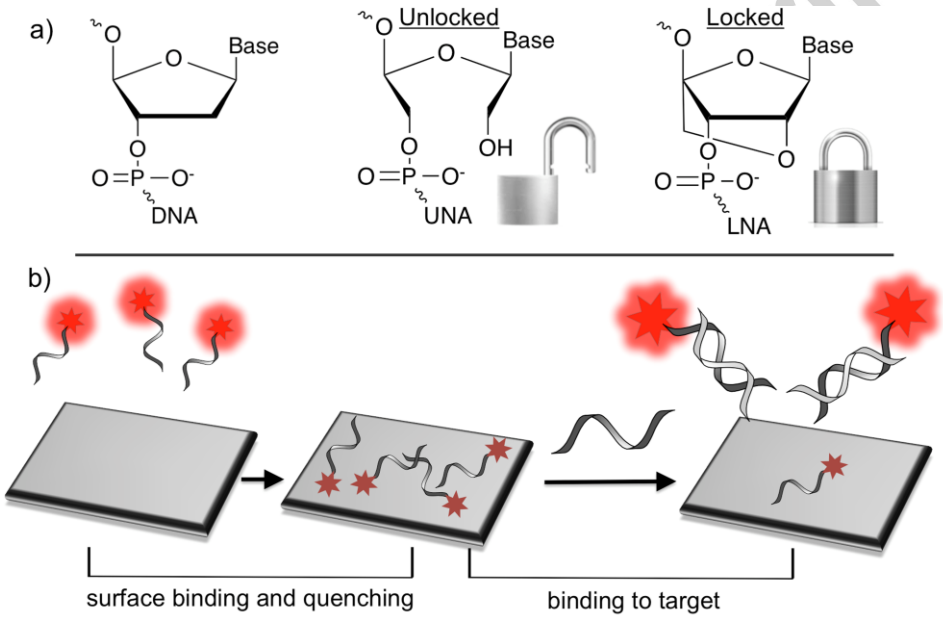

Scheme 1. (a) Illustration of DNA, UNA and LNA backbones. (b) Schematic representation of the core properties of graphene oxide that allow for miRNA detection.

Additionally, complementary oligonucleotide strands can hybridize to the surface-adsorbed probe strands and release them from the surface (Huang and Liu 2012; Wu et al. 2011). Second, the fluorescence of the probe strands, labeled with a fluorescent dye, can be quenched almost completely after adsorption onto the graphene surface, but is recoverable with hybridization induced desorption (Robertson et al. 2015b). Though these two key properties have been central for the detection of miRNAs using nGO, there are still challenges for its practical use in biomedical or biological studies such as specificity, sensitivity, and background signals (Hizir et al. 2014; Mao et al. 2013; Robertson et al. 2015a). Here we have reported our efforts to address

these challenges by inserting UNA monomers into the DNA probe strands and using a duplex-specific endonuclease.

A typical miRNA detection using nGO generally leads to a significant fluorescence recovery due to the hybridization between the surface-adsorbed fully complementary DNA molecules (probe strand) and the target miRNA. However, miRNAs with sequences similar to the target miRNA generate a non-specific fluorescence recovery, which reduces the specificity of the graphene and probe nanoassemblies (Robertson et al. 2015b). Furthermore since the generated signal is due to the hybridization between one target miRNA and one probe, the sensitivity is another critical challenge to overcome. Recently, we have addressed some of the specificity and sensitivity issues by (1) purposefully inserting mismatches into specific positions on DNA probe strands to better discriminate a single nucleotide difference and (2) utilizing the *DNase I* enzyme to amplify the overall observed signal (Robertson et al. 2015b). However, though purposefully inserting mismatches increased the specificity, it decreased the overall recovered signal, and the use of *DNase I* increased the sensitivity, but also resulted in an undesired background fluorescence increase.

In this report, we have demonstrated that incorporation of two UNA monomers into a DNA probe improved its specificity against a target miRNA more than 50 fold without sacrificing the observed fluorescence signal. Additionally, amplifying the signal intensity using a highly specific endonuclease, *dsDNase*, improved the sensitivity without affecting the background signal. Our results demonstrate that the underutilized UNAs possess remarkable potential in miRNA research and, in combination with the highly specific *dsDNase* enzyme, can be used to engineer sensitive, selective and easy-to-operate two-dimensional nanodevices for miRNA detection. Since miRNAs are considered promising tumor biomarkers for the diagnosis and prognosis of several diseases, including many types of cancer, highly sensitive and selective easy-to-use detection tools for miRNAs are in high demand. In this report we have utilized nGO, UNA probes and *dsDNase* to build potential diagnostic nanodevices for detecting and discriminating a clinically important miRNA, miR-10b (Yigit et al. 2013).

2. Materials and Methods

2.1. Materials. The following DNA and RNA sequences were purchased from Integrated DNA Technologies (IDT, USA):

(1) FAM-labeled full complementary probe (DNA_{full}), 5'-/FAM/CACAAATTCGGTTCTACAGGGTA-3'

(2) FAM-labeled probe with two UNA bases (UNA_2), 5'-/FAM/CACAA/iUNA-A/TTCGGTTCTA/iUNA-C/AGGGTA-3'

(3) FAM-labeled probe with two mismatches (DNA_{M2}), 5'-/FAM/CACAAAATCGGTTCTACAGCGTA-3'

(4) miR-10b, 5'-UACCCUGUAGAACCGAAUUUGUG-3'

(5) miR-10a, 5'-UACCCUGUAGAUCCGAAUUUGUG-3'

(6) miR-10c, 5'-UACCCUGUAGAUCCGGAUUUGU-3'

Underlined bases in (5) miR-10a and (6) miR-10c signify the nucleobase differences when compared to miR-10b. iUNA-A and iUNA-C are the unlocked nucleic acid monomers of the A and C nucleobases, respectively, inserted in the DNA probe.

dsDNase was purchased from Thermo Fisher Scientific (Waltham, MA, USA). A carboxyl graphene oxide (**Fig. S4**) water dispersion was purchased from ACS Material (Medford, MA, USA) and sonicated 12 h before use to obtain a water-soluble nanosized graphene oxide (nGO) solution. The average particle size and zeta potential were determined to be 283.3 ± 15 nm and -23.7 ± 2.9 mV, respectively, using a Malvern Instruments Zetasizer Nano ZS. RNase-free water was used for the preparation of all solutions.

2.2. Methods.

2.2.1. Effect of UNA modifications on miRNA detection and discrimination. The initial fluorescence measurements with target RNA molecules (miR-10b, miR-10a or miR10c) were performed using nanoassemblies of nano-graphene oxide (nGO) and FAM labeled antisense DNA molecules as probe strands (DNA_{full}, UNA_2 or DNA_{M2}). The nanoassemblies were prepared by mixing 50 nM probe strands with 3 µg/mL nGO in 10 mM Tris-HCl buffer (pH 7.5, 2.5 mM $MgCl_2$, 0.1 mM $CaCl_2$). Briefly, the 50 nM of probe strands was obtained by diluting a 1 µM stock solution in the Tris-HCl buffer. To each 100 µL of 50 nM probe solution, 1.50 µL of nGO stock solution (200 µg/mL) was added. This nGO addition resulted in immediate fluorescence quenching, decreasing the signal intensity by ~95% with a loading capacity of 16.7 nmol/mg (probe/nGO) and formed a highly stable biosensor. Observed fluorescence measurements were performed immediately after sample preparation using a microplate reader. Initial readings were recorded for ten minutes and later 5.0 µL of a 1 µM (50 nM final) stock

solution of miR-10b, miR-10a or miR-10c was added to the nGO/DNA_{full}, nGO/UNA_2 or nGO/DNA_{M2} nanoassemblies. A 1.5 hour kinetic study was performed to monitor the observed fluorescence and recovery kinetics at 37 °C. To determine the efficacy of higher temperature runs for miRNA detection the experiments were performed at 45 °C.

2.2.2. Determination of T_m for miRNA and probe duplexes. The melting temperatures with target RNA molecules (miR-10b, miR-10a or miR-10c) were obtained using the DNA_{full}, UNA_2 or DNA_{M2} probes. A miRNA/probe heteroduplex was prepared by mixing 1 µM probe with 1 µM target miRNA in 10 mM Tris-HCl buffer (pH 7.5, 2.5 mM $MgCl_2$, 0.1 mM $CaCl_2$). Melting curves and temperatures were obtained using a Cary 100 UV-Vis spectrophotometer with the multichannel and temperature control accessories. Measurements were performed in 3 cycles from 25 °C to 75 °C with a 1 °C/min ramp up and cool down.

2.2.3. Activity of *dsDNase* and *DNase I* on surface-adsorbed probes. To monitor the effect of *dsDNase* alone on nGO, the nanoassemblies were prepared as described above. Initial measurements were recorded for ten minutes and then 1, 2.5, or 5 µL of stock *dsDNase*, equivalent to 2U, 5U or 10U of enzymatic activity respectively, was added to each well. A 1.5 hour kinetic study was performed after the addition of the enzyme to monitor the observed fluorescence. The studies were also carried out with *DNase I* (2U, 5U or 10U) under the same experimental conditions to monitor and compare the enzymatic activity on the surface.

2.2.4. Signal enhancement using *dsDNase*. For monitoring the effect of *dsDNase* on the miRNA for signal amplification, the probes (DNA_{full}, UNA_2 or DNA_{M2}) were first adsorbed onto the nGO surface as described above. After initial readings without any miRNA addition were recorded, 2 µL of stock *dsDNase* was added to the 100 µL of each nanoassembly. Ten minutes after the addition of the enzyme, 5 µL of a 1 µM stock (50 nM final concentration) target miRNA (miR-10b, miR-10a, or miR-10c) was added to each well. The studies were also carried out with various concentrations (10, 20, 30, 40 and 50 nM) of miR-10b. A 1.5 hour kinetic study was performed to monitor the observed fluorescence and recovery kinetics.

2.2.5. Fluorescence measurements. Fluorescence measurements were performed using a BioTek Synergy H1 microplate reader. The fluorescence of the FAM (ext: 495 nm, em: 520) label was monitored during the kinetic measurements by either nonstop reading or end-point reading. The samples were excited at 485 nm and the emission was collected at 520 nm. The

gain value was set to 100 for each reading. The temperature was set to 37 or 45 °C for different experimental setups. Fluorescent images were taken using a Bio-Rad ChemiDoc.

2.2.6. Statistical Analysis. Data are expressed as mean ± SD. Statistical differences were analyzed by the Student's t-test (http://graphpad.com). Experiments were performed in triplicate.

3. Results and Discussion

First we compared the melting temperatures of DNA_{full} and UNA_2 with the fully complementary RNA strand, miR-10b. The results demonstrate that insertion of two UNAs decreased the melting temperature about 11 °C, **Figs. 1a and b**. Since our goal in this study is to detect miR-10b and discriminate it from miR-10a and miR-10c, we have also monitored the melting temperatures with these two miRNAs. Similarly, the melting temperature for the UNA_2 and miR-10a duplex was determined to be 14 °C lower than the DNA_{full} and miR-10a duplex. Furthermore the melting temperature data between UNA_2 and miR-10c did not provide a standard melting curve due to the lack of interaction between the two strands. We hypothesized

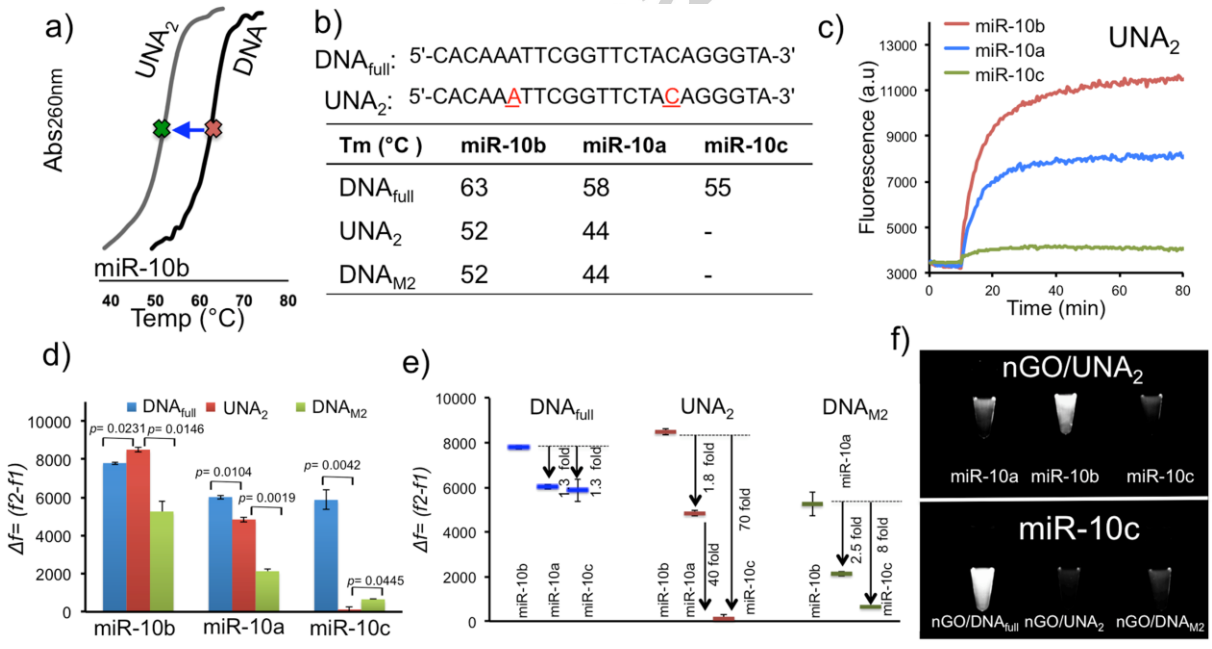

Fig. 1. (a) Decrease (11 °C) in the melting temperature of the DNA probe with the insertion of two UNA monomers. (b) Sites of UNA insertions (red) and melting temperatures of probes with miR-10b, miR-10a and miR-10c. (c) Fluorescence recovery curves with mi-10b, miR-10a and miR-10c using nGO/UNA_2 nanoassemblies at 37 °C. (d-e) Fluorescence signals observed with the nGO/DNA_{full}, nGO/UNA_2 or nGO/DNA_{M2} and miRNA targets at the end of 90 minutes of incubation at 37 °C. (f) Fluorescent images comparing the specificity of the nGO/UNA_2 recovery with all target miRNAs and two other nanoassemblies at 37 °C.

that the lower melting temperatures and instability of the duplexes with UNA_2 can enable us to discriminate miR-10b from miR-10a and miR-10c using two-dimensional nano-graphene oxide (nGO).

We first assembled the fluorescently silent nanoassemblies using nGO and the DNA_{full}, UNA_2 and DNA_{M2} probes, separately. The DNA_{M2} probe has two mutations inserted at specific positions of the fully complementary DNA_{full} probe. DNA_{M2} is mutated at the 7th and 20th bases from the 5′ end of DNA_{full} by replacing the T base with A (T→A)[7] and the G base with C (G→C)[20], respectively. These mutations did not affect the adsorption efficiency of the probes on the nGO surface as observed by a similar magnitude of fluorescence quenching with each probe, **Figs. 1b and S1**. As reported in our recent paper, the DNA_{M2} probe was superior to the full complementary probe for the discrimination of miR-10b from miR-10a, which differs by only a single nucleotide (Robertson et al. 2015b). On the other hand, insertion of these two mutations sacrificed the overall observed signal with the target strand. In this study, DNA_{M2} was used to evaluate and compare the affinity of UNA_2 for the detection and discrimination of miR-10b.

The fluorescence recovery curves were obtained using miR-10b, miR-10a and miR-10c with the nGO/DNA_{full}, nGO/UNA_2 or nGO/DNA_{M2} nanoassemblies, **Figs. 1c and S1**. As predicted, miR-10b resulted in a higher fluorescence recovery than miR-10a and miR-10c using all three nanoassemblies, **Fig. 1d**. The observed fluorescence signals with miR-10b using nGO/UNA_2 and nGO/DNA_{full} were equally high and statistically not very significant. On the other hand, the miR-10b signal observed with nGO/DNA_{M2} was significantly lower than those of nGO/UNA_2 and nGO/DNA_{full}. The results indicate that insertion of UNA monomers into the probe strands does not sacrifice the observed fluorescence signal for target miRNA detection. Later the discrimination of miR-10b from miR-10a and miR-10c was evaluated using all three nanoassemblies, **Fig. 1e**. The observed fluorescence signal for miR-10b was only about 1.3 fold greater than that of both miR-10a and miR-10c using nGO/DNA_{full}. However, these values were 1.8 and 70 fold for miR-10a and miR-10c using nGO/UNA_2. Furthermore, the observed signal with miR-10c was 40 fold less than miR-10a using nGO/UNA_2, which was only about 1.0 using nGO/DNA_{full}. The results suggest that UNA_2 is 50 times more efficient than DNA_{full} for discriminating miR-10b from miR-10c. The observed fluorescence signal using nGO/DNA_{M2} for detection of miR-10b was 2.5 and 8 fold greater than that of miR-10a and miR-10c, respectively.

Even though the discrimination of miR-10b from miR-10a is slightly better using nGO/DNA_{M2} compared to nGO/UNA_2, the signal observed with the target miR-10b is decreased dramatically when using nGO/DNA_{M2}, while such a loss in signal was not observed with nGO/UNA_2, **Fig. 1e**. Finally, fluorescent images of the nGO/UNA_2 nanoassemblies with each miRNA, and all three nanoassemblies with miR-10c, suggest that nGO/UNA_2 offers remarkable discrimination between miR-10b and miR-10c, and is superior to that of nGO/DNA_{full} and nGO/DNA_{M2}, **Fig. 1f**. Our studies also demonstrated that even though the incorporation of either mismatches or UNA monomers resulted in the same degree of decrease in the melting temperatures of the duplexes, the nGO/UNA_2 improved the fluorescence recovery slightly when compared to nGO/DNA_{full} whereas nGO/DNA_{M2} diminished the fluorescence recovery, **Figs 1b and d**. This observation could be due to the difference in the interaction between the nGO surface and the ss DNA molecules with and without UNA modifications. UNA monomers introduced into the DNA backbone increase its flexibility and therefore can impact the interaction between nucleobases and the nGO surface, which could be observed as a greater release from the surface after binding to a target strand.

After demonstrating the effectiveness of the nGO/UNA_2 complex for discriminating a single and double nucleotide difference, we moved our focus to optimizing the temperature range for detection. By inserting the UNAs into our probe strand, our aim was to destabilize the duplex formation with non-target strands (miR-10a and miR-10c) at elevated temperatures. To measure the melting temperatures, we prepared six different probe mixes, using 1 µM of each of the probe strands (DNA_{full}, UNA_2 or DNA_{M2}) and 1 µM of either miR-10b or miR-10a, and measured the absorbance from 25 to 75 °C, **Fig. S2**. The melting temperatures obtained with UNA_2 were significantly lower than the DNA_{full} and roughly equal to those of the DNA_{M2} probe, which fell at 52 °C and 44 °C for miR-10b and miR-10a, respectively, **Fig. 2a**. These results reinforced the idea that a better discrimination between miR-10b and miR-10a could be obtained by running the detection at a temperature lower than 50 °C and higher than 44 °C.

Based on these results, we decided to move to a temperature of 45 °C which was closer to the melting temperature of our UNA_2 probe with miR-10a, and greater than that of miR-10c, while maintaining a stable duplex with miR-10b. Though this increase in temperature could have been performed with the full complementary probe and the 6 °C difference between targets, the

incorporation of the UNAs was exceptionally important to bring the duplex melting temperature into our enzyme's active range, which was used for signal amplification studies as mentioned below. This is one of the reasons why UNAs are important for miRNA detection: they allow for the tuning of the working temperature range by manipulating the melting temperatures of the heteroduplexes without sacrificing the amplitude of observed fluorescence signal.

First the kinetics study was performed at 45 °C to monitor the fluorescence recovery with all three miRNAs using all three nanoassemblies, **Fig. 2b and S3**. As seen, miR-10c gives almost only background signal using nGO/UNA_2 while miR-10b and miR-10a result in a fast fluorescence recovery. Later, observed fluorescence signals were recorded at 37 and 45 °C for miR-10b, miR-10a and miR-10c using all three nanoassemblies, **Figs. 2c and S3**. As predicted, the fluorescence recoveries with miR-10a decreased significantly at 45 °C using nGO/UNA_2 and nGO/DNA_{M2} while the change with nGO/DNA_{full} was not statistically different. Furthermore the

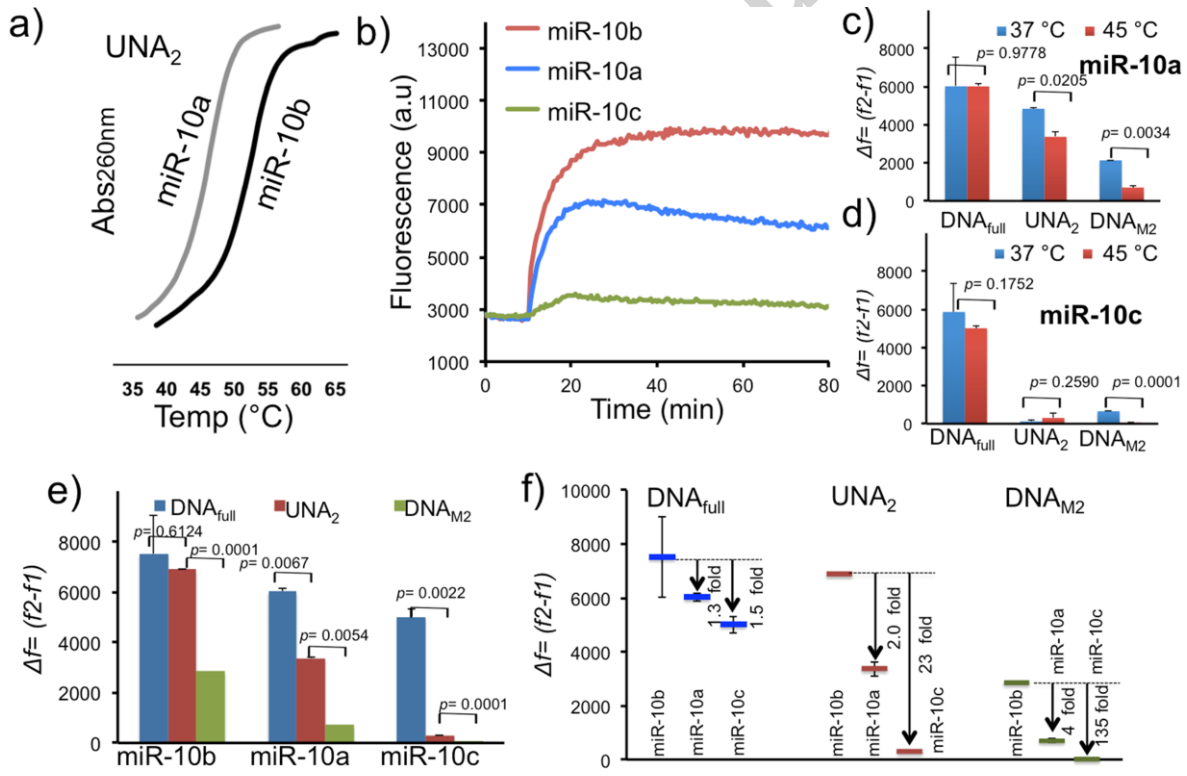

Fig. 2. (a) Difference in the melting temperatures of miR-10b and miR-10a with UNA_2. (b) Fluorescence recovery curves with miR-10b, miR-10a and miR-10c using nGO/UNA_2 nanoassemblies. Final observed fluorescence at the end of 90 minutes of incubation with nGO/DNA_{full}, nGO/UNA_2 or nGO/DNA_{M2} at 45 °C and (c) miR-10a or (d) miR-10c at 37 °C and 45 °C. (e-f) Fluorescence signals observed with the nGO/DNA_{full}, nGO/UNA_2 or nGO/DNA_{M2} and miRNA targets at the end of 90 minutes of incubation at 45 °C.

signals obtained with miR-10c were almost at background levels using nGO/UNA_2 and nGO/DNA_{M2} at both temperatures, however there was still very significant fluorescence recovery using the nGO/DNA_{full}, **Fig. 2d**. Comparison between the observed fluorescence signals suggests that in contrast to the nGO/DNA_{full} and nGO/DNA_{M2} nanoassemblies, nGO/UNA_2 provides very high fluorescence signal with the target miRNA, miR-10b (not statistically different than nGO/DNA_{full}), while offering a greater discrimination over off-targets, miR10a and miR-10c, **Figs. 2e and 2f**.

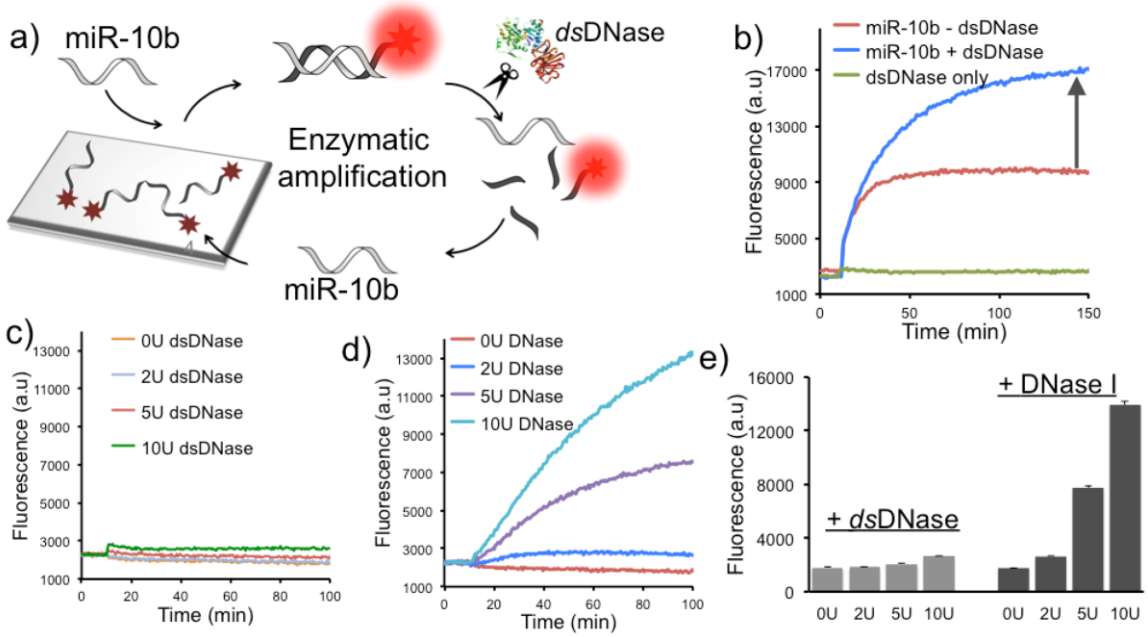

Fig. 3. (a) Illustration of the amplification of the fluorescence using *dsDNase*. (b) Fluorescence recovery curves using nGO/UNA_2 with miR-10b and *dsDNase*, miR-10b without *dsDNase*, and *dsDNase* alone at 45 °C. The digestion of UNA_2 probes in the nGO/UNA_2 nanoassemblies with different amounts of (c) *dsDNase* and (d) *DNase I* over time. (e) Final fluorescence signals with different amounts of *dsDNase* and *DNase I* at the end of 90 minutes of incubation.

Building off of the results of the UNAs for increasing the specificity against the target miRNA, we moved forward to amplify the observed fluorescence signals using an endonuclease. The endonucleases have been used for enhancing the miRNA-induced signal recovery by cleaving the phosphodiester backbone of the DNA probes in the miRNA/DNA helices (Xi et al. 2014; Yin et al. 2012). The fragmented DNA probes, including the fluorescent labels, are released into the solution without adsorbing back onto the graphene surface while the freed miRNA recycles and binds to another surface-adsorbed probe. As a result, one miRNA can

release and induce the cleavage of multiple probe stands, **Fig. 3a**. We have recently used *DNase I* for signal amplification, however discovered that it also degrades the surface-adsorbed ss DNA probes resulting in a background fluorescence increase. In order to avoid this undesired activity of *DNase I,* and therefore the background fluorescence increase, our nanodevice surface was modified with PEGMA polymers using a long and complicated multi-step procedure (Robertson et al. 2015a; Robertson et al. 2015b). In order to amplify the fluorescence signal and overcome the background signal, without the labor-intensive surface modification procedure with polymers, in this study we utilized a duplex specific endonuclease, *dsDNase*, enzyme instead *DNase I*. *dsDNase* is an enzyme which specifically cleaves the phosphodiester backbone of DNA molecules only when they are in a DNA:RNA or DNA:DNA duplex. In contrast to the others reported in the literature (Yin et al. 2012), the *dsDNase* functions under physiological conditions where short miRNA:DNA probe duplexes can remain stable.

First we tested whether *dsDNase* can amplify the signal with miR-10b using nGO/UNA_2. As seen in **Fig. 3b**, the observed fluorescence signal recorded for miR-10b only (red curve) is amplified when in the presence of *dsDNase* (blue curve). Furthermore, when *dsDNase* was used alone, without any miRNA addition, no fluorescence signal recovery was observed using nGO/UNA_2, which suggests that *dsDNase* has no activity on surface adsorbed probe strands. To examine the surface activity of the *dsDNase* enzyme thoroughly, comparable volumes of each enzyme, *DNase I* and *dsDNase*, were added to nGO/UNA_2 nanoassemblies alone. Due to the exceptionally high specificity of *dsDNase* towards duplex molecules only, no enzymatic activity of the *dsDNase* was observed on the surface adsorbed ss probe strands even at as high as 10U of enzymatic activity, **Figs. 3c and 3e**. On the other hand, *DNase I* cleaved the surface adsorbed ss probe strands resulting in a significant background increase with various concentrations of the enzyme, **Figs. 3d and 3e**. These results strongly supported the use of *dsDNase* over *DNase I* for amplifying the signal recovery, which will only be due to the cleavage of the probe strands in the miRNA:UNA_2 duplexes.

With our results suggesting the nGO/UNA_2 nanoassembly's capability for specific detection so far, we moved to test the complete system with the discrimination of three miRNAs. By incorporating the *dsDNase* enzyme into the reaction mixture, a significant increase in the recovered fluorescence was observed, **Fig. 4a**. miR-10b addition resulted in the highest

fluorescence with all three nanoassemblies followed by miR-10a and then miR-10c, respectively. In contrast to the nGO/DNA_{full} and nGO/DNA_{M2} nanoassemblies, nGO/UNA_2 provided a better discrimination between each miRNA while maintaining the high fluorescence signal with the target strand. Also, when compared to the enzyme free studies the observed fluorescence signals are almost doubled in the presence of *dsDNase*, **Fig. 4a**. The fluorescence readings were also recorded for different concentrations of miR-10b using nGO/UNA_2 and *dsDNase*, **Fig. 4b**.

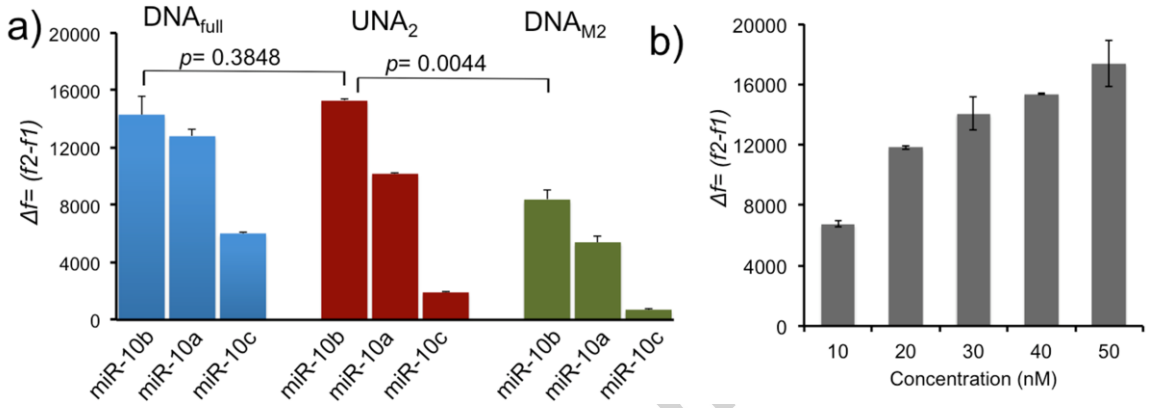

Fig. 4. (a) Observed fluorescence signals with miR-10b, miR-10a and miR-10c using *dsDNase* with the nGO/DNA_{full}, nGO/UNA_2 or nGO/DNA_{M2} nanoassemblies at the end of 90 minutes of incubation at 45 °C. (b) Observed fluorescence readings with various concentrations of miR-10b using nGO/UNA_2 and *dsDNase*.

4. Conclusion

Here we have investigated how the combination of the underutilized UNAs and *dsDNase* can give more control in the detection of miRNAs using water-soluble nano-graphene oxide nanoassemblies. We have demonstrated that by strategic placement of UNAs within probe sequences, a greater specificity was observed towards a target RNA, miR-10b, over two other RNAs within the same family, which differ by as little as a single nucleotide. We observed a 70 fold higher fluorescence signal for the target miRNA, miR-10b, over miR-10c which has only a two nucleobase difference. Moreover, with the addition of the highly DNA specific endonuclease *dsDNase*, which only cleaves DNA:DNA or RNA:DNA duplexes, we were able to enhance the resulting signal intensity. This study demonstrates that the challenges in miRNA detection may be addressed with the UNAs and endonucleases, and by combining several of these approaches a more robust detection is possible. Though our method in this work was only used to increase the specificity towards miR-10b, the same combination of approaches may be used for the detection of other miRNAs of interest.

5. References

Allen, M.J., Tung, V.C., Kaner, R.B., 2010. Chem. Rev. 110(1), 132-145.

Balci, O., Polat, E.O., Kakenov, N., Kocabas, C., 2015. Nat. Commun. 6, 6628.

Balcioglu, M., Rana, M., Yigit, M.V., 2013. J. Mater. Chem. B 1(45), 6187-6193.

Butun, S., Tongay, S., Aydin, K., 2015. Nano Lett. 15(4), 2700-2704.

Campbell, M.A., Wengel, J., 2011. Chem. Soc. Rev. 40(12), 5680-5689.

Chung, C., Kim, Y.K., Shin, D., Ryoo, S.R., Hong, B.H., Min, D.H., 2013. Acc .Chem. Res. 46(10), 2211-2224.

Dreyer, D.R., Park, S., Bielawski, C.W., Ruoff, R.S., 2010. Chem. Soc. Rev. 39(1), 228-240.

Elmen, J., Lindow, M., Schutz, S., Lawrence, M., Petri, A., Obad, S., Lindholm, M., Hedtjarn, M., Hansen, H.F., Berger, U., Gullans, S., Kearney, P., Sarnow, P., Straarup, E.M., Kauppinen, S., 2008. Nature 452(7189), 896-899.

Geim, A.K., 2009. Science 324(5934), 1530-1534.

Guo, Q., Zhu, H., Liu, F., Zhu, A.Y., Reed, J.C., Yi, F., Cubukcu, E., 2014. ACS Photonics 1(3), 221-227.

Hizir, M.S., Balcioglu, M., Rana, M., Robertson, N.M., Yigit, M.V., 2014. ACS Appl. Mater. Interfaces 6(17), 14772-14778.

Huang, P.J., Liu, J., 2012. Anal. Chem. 84(9), 4192-4198.

Jensen, T.B., Langkjaer, N., Wengel, J., 2008. Nucleic Acids Symp Ser (Oxf)(52), 133-134.

Langkjaer, N., Pasternak, A., Wengel, J., 2009. Bioorg. Med. Chem. 17(15), 5420-5425.

Mai, C., Barrette, A., Yu, Y., Semenov, Y.G., Kim, K.W., Cao, L., Gundogdu, K., 2014. Nano Lett. 14(1), 202-206.

Mao, H.Y., Laurent, S., Chen, W., Akhavan, O., Imani, M., Ashkarran, A.A., Mahmoudi, M., 2013. Chem. Rev. 113(5), 3407-3424.

Nielsen, P., Dreiøe, L.H., Wengel, J., 1995. Bioorg. Med. Chem. Lett. 3(1), 19-28.

Ocsoy, I., Gulbakan, B., Chen, T., Zhu, G., Chen, Z., Sari, M.M., Peng, L., Xiong, X., Fang, X., Tan, W., 2013. Adv. Mater. 25(16), 2319-2325.

Ozturk, B., de-Luna-Bugallo, A., Panaitescu, E., Chiaramonti, A.N., Liu, F., Vargas, A., Jiang, X., Kharche, N., Yavuzcetin, O., Alnaji, M., Ford, M.J., Lok, J., Zhao, Y., King, N., Dhar, N.K., Dubey, M., Nayak, S.K., Sridhar, S., Kar, S., 2015. Sci. Adv. 1(6).

Parlak, O., Tiwari, A., Turner, A.P., Tiwari, A., 2013. Biosens. Bioelectron. 49, 53-62.

Parlak, O., Turner, A.P., Tiwari, A., 2014. Adv. Mater. 26(3), 482-486.

Parlak, O., Turner, A.P.F., Tiwari, A., 2015. J. Mater. Chem. B 3(37), 7434-7439.

Pasternak, A., Wengel, J., 2010. Nucleic Acids Res. 38(19), 6697-6706.

Pasternak, A., Wengel, J., 2011. Bioorg. Med. Chem. Lett. 21(2), 752-755.

Rana, M., Balcioglu, M., Robertson, N., Yigit, M.V., 2014a. Analyst 139(4), 714-720.

Rana, M., Balcioglu, M., Yigit, M., 2014b. BioNanoScience 4(2), 195-200.

Robertson, N.M., Hizir, M.S., Balcioglu, M., Rana, M., Yumak, H., Ecevit, O., Yigit, M.V., 2015a. Bioconjugate Chem. 26(4), 735-745.

Robertson, N.M., Salih Hizir, M., Balcioglu, M., Wang, R., Yavuz, M.S., Yumak, H., Ozturk, B., Sheng, J., Yigit, M.V., 2015b. Langmuir 31(36), 9943-9952.

Vester, B., Wengel, J., 2004. Biochemistry 43(42), 13233-13241.

Wu, M., Kempaiah, R., Huang, P.J., Maheshwari, V., Liu, J., 2011. Langmuir 27(6), 2731-2738.

Xi, Q., Zhou, D.M., Kan, Y.Y., Ge, J., Wu, Z.K., Yu, R.Q., Jiang, J.H., 2014. Anal. Chem. 86(3), 1361-1365.

Yigit, M.V., Ghosh, S.K., Kumar, M., Petkova, V., Kavishwar, A., Moore, A., Medarova, Z., 2013. Oncogene 32(12), 1530-1538.

Yin, B.C., Liu, Y.Q., Ye, B.C., 2012. J. Am. Chem. Soc. 134(11), 5064-5067.

You, Y., Moreira, B.G., Behlke, M.A., Owczarzy, R., 2006. Nucleic Acids Res. 34(8), e60.

Zhu, A.Y., Yi, F., Reed, J.C., Zhu, H., Cubukcu, E., 2014. Nano Lett. 14(10), 5641-5649.

Table of Content Figure: